Supplemental online material for: Evidence for the role of proton shell closure in quasi-fission reactions from X-ray fluorescence of mass-identified fragments

M. Morjean,[1] D.J. Hinde,[2] C. Simenel,[2,*] D.Y. Jeung,[2] M. Airiau,[3,4] K.J. Cook,[2] M. Dasgupta,[2] A. Drouart,[4] D. Jacquet,[3] S. Kalkal,[2] C.S. Palshetkar,[2] E. Prasad,[2] D. Rafferty,[2] E.C. Simpson,[2] L. Tassan-Got,[3] K. Vo-Phuoc,[2] and E. Williams[2]

[1]*GANIL, CEA-DSM and IN2P3-CNRS, B.P. 55027, F-14076 Caen Cedex, France*
[2]*Department of Nuclear Physics, Research School of Physics and Engineering, The Australian National University, ACT 0200, Australia*
[3]*Institut de Physique Nucléaire, CNRS-IN2P3, Université Paris-Sud, Université Paris-Saclay, F-91406 Orsay Cedex, France*
[4]*Irfu, CEA, Université Paris-Saclay, F-91191 Gif-sur-Yvette, France*

This supplemental material gives details of the time-dependent Hartree-Fock calculations performed to investigate the quasi-fission process in the ^{48}Ti+^{238}U reaction.

THE TIME-DEPENDENT HARTREE-FOCK THEORY

The non-relativistic time-dependent Hartree-Fock (TDHF) theory is a mean-field approach to the dynamical many-fermion problem. Applied to nuclear systems, it provides an independent particle picture where each nucleon evolves in the mean-field produced by the ensemble of nucleons. The many-body state of the system is written as an antisymmetrised product (Slater determinant) of the single-particle wave-functions $\varphi_i(t)$ with occupation numbers $n_i = 1$, accounting for the Pauli exclusion principle exactly. In the TDHF theory, the system is constrained to remain in such an independent particle many-body state $\Phi(t)$ at any time t. All the information on the state of the system is then contained in the occupied single particle states $\varphi_i(t)$, or, equivalently, in the one-body density matrix $\rho(t)$ associated to $\Phi(t)$ with matrix elements

$$\rho_{\alpha\beta} = \langle\Phi|\hat{a}^\dagger_\beta \hat{a}_\alpha|\Phi\rangle, \tag{1}$$

where $\hat{a}^\dagger_\alpha$ (resp. $\hat{a}_\alpha$) creates (annihilates) a particle in the state $|\alpha\rangle$. In the coordinate basis $\{\mathbf{r}, s, q\}$, denoting position, spin and isospin of a nucleon, respectively, the one-body density matrix reads

$$\rho(\mathbf{r}sq, \mathbf{r}'s'q') = \sum_i n_i \varphi^*_i(\mathbf{r}'s'q')\varphi_i(\mathbf{r}sq). \tag{2}$$

It is assumed to be diagonal in isospin.

The TDHF equation is written as

$$i\hbar\frac{\partial}{\partial t}\rho(t) = [h[\rho], \rho], \tag{3}$$

where $h[\rho]$ is the self-consistent single-particle Hartree-Fock hamiltonian. It is derived from the energy density functional (EDF) $E[\rho]$ according to

$$h[\rho]_{\alpha\beta} = \frac{\delta E[\rho]}{\delta\rho_{\beta\alpha}}. \tag{4}$$

SKYRME ENERGY DENSITY FUNCTIONAL

We use the SLy4*d* parametrisation [1] of the Skyrme EDF. It incorporates the spin density $\mathbf{S}$ and the spin-orbit density $\mathbf{J}$, but neglects other contributions from the spin-current pseudo-tensor $\overleftrightarrow{J}$, as well as the spin kinetic energy density $\mathbf{T}$ and terms in $\mathbf{S}\Delta\mathbf{S}$ in the EDF. Note that the SLy4*d* parametrisation has been fitted without center-of-mass corrections to allow for the description of heavy-ion collisions (see [2] for more details).

In its original version, the TDHF theory neglects pairing residual interaction. However, to improve the convergence of the static mean-field calculation of the collision partners, the pairing correlations are included at the BCS (Bardeen-Cooper-Schrieffer) level. The resulting distribution of single-particle occupation numbers is kept frozen in the time evolution ("frozen occupation approximation"). The pairing interaction acts in the $^1S_0$ channel in an energy window of ± 5 MeV around the Fermi level. We chose a density-dependent parametrisation defined as

$$\hat{v}^{pair}(\mathbf{r}, \mathbf{r}') = -\frac{V_0}{2}\left(1 - \hat{P}_\sigma\right)\left[1 - \frac{\rho(\mathbf{r})}{\rho_0}\right]\delta(\mathbf{r} - \mathbf{r}'), \tag{5}$$

where $\rho(\mathbf{r})$ is the nucleon density, $\rho_0 = 0.16$ fm^{-3}, and $V_0 = 1000$ MeV·fm^{-3} for both protons and neutrons.

NUMERICAL DETAILS

We use a modified version of the TDHF3D code [1]. Details of the algorithm used to solve the TDHF equation (3) can be found in Ref. [2]. The HF+BCS and TDHF calculations are solved in a cartesian grid with mesh size $\Delta x = 0.8$ fm. Both collision partners are initially in their HF+BCS ground-states, with a distance of 33.6 fm between the centers of mass, in a box with dimension $(84 \times 28 \times 28/2)\Delta x^3$. The code assumes a $z = 0$ plane of symmetry (hence the factor $1/2$ in the box size). The time evolution is performed with a time step $\Delta t = 1.5 \times 10^{-24}$ s.

To save computational time, all calculations are performed for central collisions. Two initial orientations of the deformed

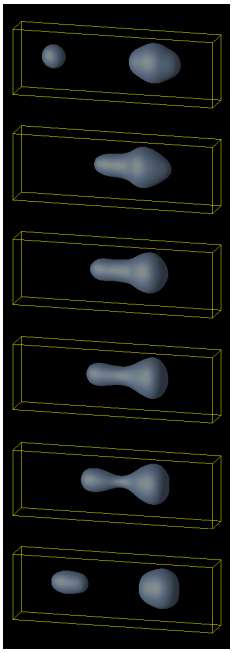

FIG. 1. Evolution of the isodensity at half the saturation density, $\rho_0/2 = 0.08$ fm^{-3}, every 1.5×10^{-21} s, for the ^{48}Ti+^{238}U central collision with the tip orientation at a center of mass energy of 230 MeV.

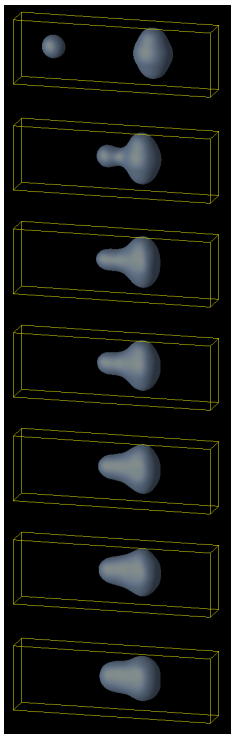

FIG. 2. Same as Fig. 1 for the side orientation.

TABLE I. Expectation value of the mass, neutron and proton numbers of the heavy fragment produced in ^{48}Ti+^{238}U central collisions with the tip orientation at various center of mass energies.

$E_{c.m.}$	A	N	Z
170	237.97	145.97	92.00
175	237.95	145.95	92.00
180	237.93	145.92	92.01
185	237.88	145.85	92.04
190	237.76	145.56	92.20
195	236.65	144.02	92.63
200	232.97	141.77	91.19
205	196.64	119.00	77.65
210	209.42	127.04	82.37
215	209.86	127.51	82.35
220	210.96	128.05	82.91
225	211.03	127.99	83.04
230	210.58	127.65	82.94

TABLE II. Same as Table I for the side orientation.

$E_{c.m.}$	A	N	Z
200	237.79	145.76	92.04
205	237.65	145.55	92.10
210	237.57	144.98	92.58
215	236.35	143.55	92.79
216	235.70	143.20	92.50
217	235.04	142.71	92.33
218	234.86	142.51	92.35
219	235.47	142.86	92.61
220	234.99	142.77	92.21
221	234.58	142.55	92.03
222	233.96	142.18	91.78
223	228.63	138.63	90.00
224	215.97	131.01	84.96
225		Fusion	
230		Fusion	

^{238}U are considered: the "tip" orientation where the deformation axis of ^{238}U is parallel to the collision axis (see top panel of Fig. 1), and the "side" orientation where they are perpendicular (see top panel of Fig. 2). Instead of varying the impact parameter at a fixed energy, we vary the energy, from the maximum center of mass energy $E_{c.m.}$ of 230 MeV down to 200 MeV (170 MeV) for the side (tip) orientation (in steps of 5 MeV). We performed additional calculations for the side orientation between 215 and 225 MeV in 1 MeV step. The variation of energy allows to span a large range of distances of closest approach leading to various contact times and hence various amount of nucleon transfer. Similar variation in distances of closest approach could be obtained by varying the impact parameter. However, this would require much larger boxes (and thus an increase of the computational time) to account for all possible trajectories in the reaction plane.

RESULTS

Figures 1 and 2 show the resulting time evolution of the density for the tip and side orientations, respectively, at a center of mass energy of 230 MeV. The maximum simulation time considered in this work is 9×10^{-21} s (with the exception

of the side orientation at $E_{c.m.} = 224$ MeV which led to quasifission at the end of a 12×10^{-21} s simulation). We call "fusion" reactions which lead to a single compact fragment after this time, as in the lowest panel of Fig. 2, although the system could eventually encounter subsequent reseparation corresponding to long-time quasifission.

As in previous quasifission studies with TDHF [2–6], fusion is only observed for the highest energies with the side orientation. All tip collisions lead to a reseparation in two fragments before the end of the calculation. A summary of the N and Z of the heavy fragment formed at the different energies is given in Tables I and II for the tip and side orientations, respectively.

* cedric.simenel@anu.edu.au

[1] Ka–Hae Kim, Takaharu Otsuka, and Paul Bonche, J. Phys. G **23**, 1267 (1997).
[2] C. Simenel, Eur. Phys. J. A **48**, 152 (2012).
[3] A. Wakhle, C. Simenel, D. J. Hinde, M. Dasgupta, M. Evers, D. H. Luong, R. du Rietz, and E. Williams, Phys. Rev. Lett. **113**, 182502 (2014).
[4] V. E. Oberacker, A. S. Umar, and C. Simenel, Phys. Rev. C **90**, 054605 (2014).
[5] A. S. Umar, V. E. Oberacker, and C. Simenel, Phys. Rev. C **94**, 024605 (2016).
[6] K. Sekizawa and K. Yabana, Phys. Rev. C **93**, 054616 (2016).